Operation Capability Analysis and Experiments of Underactuated Compliant Multi-Fingered Hands

Shun Xiao[*,#], Jiejian Di[#], Jie Zhang, Quanliang Zhao and Guangping He

Department of Mechanical and Electrical Engineering, North China University of Technology, Beijing, 100144, P.R., China

Abstract: In this paper, operation capabilities of underactuated compliant robot hands have been investigated based on the shape stability analysis of underactuated compliant fingers and operation modes analysis of human hands. It is shown that the operation modes of robot hands can be classified into two major classes, namely, enveloping grasp mode and pinch mode. For the two operation modes, two principles are respectively presented with regard to the mechanical design issues of the underactuated robot hands. According to the principles presented in this paper, a robot hand prototype with four underactuated compliant fingers has been fabricated. On the robot hand prototype, enveloping grasp capability of underactuated compliant robot hands has been verified by many experiments. For precision operations, a proposition is presented and it is shown that the prototype should be further improved.

Keywords: Underactuation, Robot hands, Prototype, Compliancy, Enveloping grasp.

1. INTRODUCTION

In order to reduce the cost of the systems and promote the extensive applications of multi-fingered robot hands, underactuated multi-fingered robot hands have been given many investigations in robotics field in recent years [1-10]. Different from the concept of underactuation in dynamical robotic systems such as underactuated manipulators [11], underactuated surface vehicles [12], dynamically legged robot systems [13], and underactuated gyroscopes [14] etc., of which the static equilibrium configurations are generally not stable since some free passive degrees of freedom (DOF) are involved in the mechanisms or the systems only work in dynamical mode, the underactuated multi-fingered hands [1] generally belong to a class of low-speed manipulation systems, of which the static equilibrium configurations are stable since the passive DOF of the mechanisms are generally installed elastic elements [4].

Since the number of independent actuators is less than that of the DOF of the mechanisms, the controllability of underactuated mechanisms is an important issue in practical applications [15]. For the underactuated mechanical systems with free passive DOF, the controllability of the systems is a difficult problem since the systems are generally high-order nonholonomic systems [11, 16]. However, for the underactuated mechanical systems with elastic passive DOF [2-4], the controllability of the systems can be guaranteed by mechanical design, even though that is generally based on the intuitions of the designers [5], thereby some full-actuated robot hands with reduced DOF in mechanisms in some literatures are mistakenly called underactuated robot hands [5]. In this paper, the *underactuated multi-fingered robot hands* are defined as robot hands with *elastic passive DOF* in mechanisms. In other words, there are some passive DOF in the mechanisms whereas the passive DOF are indirectly actuated by elastic elements [6-8], such as springs and compliant linkages, so that all of the static equilibrium configurations of the underactuated mechanisms are controllable and locally stable.

To clarify this definition, let's see Figures **1** and **2**, which show two major classes of mechanisms that are commonly used in underactuated multi-fingered hands. The Figure **1a** illustrates a linkage-based finger mechanism actuated by single actuator [1]. Though there are three phalanxes in the mechanism, the mechanism is full actuated since the number of DOF of the mechanism is one. When we want to design an underactuated finger by the linkage-based mechanism and at the same time the controllability of the mechanism is guaranteed, then at least one elastic passive DOF should be introduced into the mechanism (see Figure **1b**), and the stiffness of the elastic element should be large enough, so that the movements of the mechanism are stable for certain loads.

Figure **2** shows another class of mechanisms commonly used in designing the fingers of robot hands. The Figure **2a** shows a full actuated and tendon-pulley based mechanism [17, 18], which is similar to the linkage-based mechanism shown in Figure **1a**. When we want to design an underactuated mechanism based

Address correspondence to this author at the Department of Mechanical and Electrical Engineering, North China University of Technology, Beijing, 100144, P.R., China; Tel: 86-010-88802835; E-mail: 17726294905@163.com

[#]These contributed equally to this work.

E-ISSN: 2409-9694/20 © 2020 Zeal Press

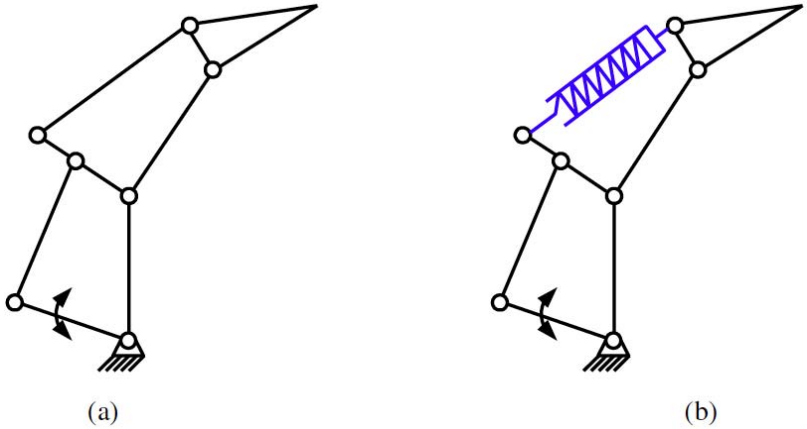

Figure 1: Linkage-based finger mechanisms of robot hands.

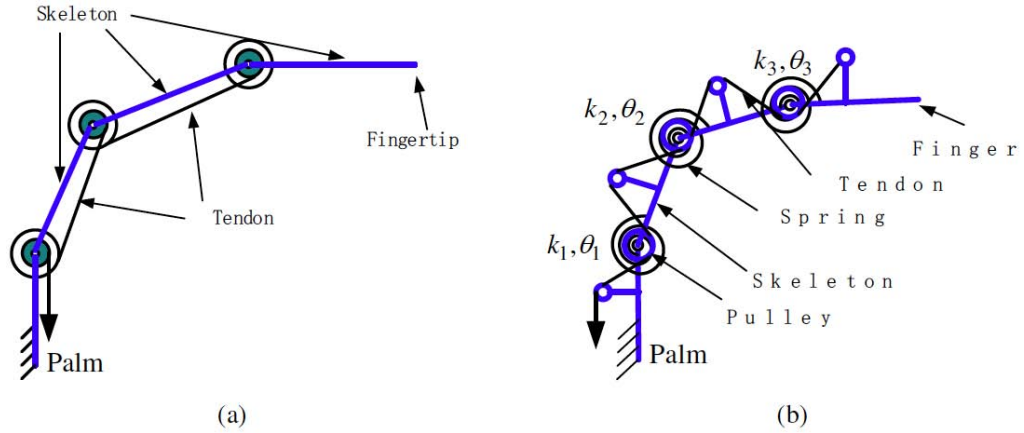

Figure 2: Tendon-pulley based finger mechanisms of robot hands.

on the tendon-pulley transmission system, we should use single tendon instead of several ones so that the joint angles of the phalanxes can be independently changed. It is worth pointing out that the joint angles of the mechanisms shown in Figures **1a** and **2a** are obviously determined by an algebraic equation with single angular variable of the driving linkage. Thus, they are actually full-actuated mechanisms.

From Figures **1** and **2**, it can be concluded that the configurations of a full-actuated finger mechanism are determined by the position of the driving linkage, while the configurations of an underactuated finger mechanism with elastic passive DOF are determined by both the actuation force and the external resistance forces. As shown in Figure **3**, a robot hand with underactuated fingers will have more contacting points between the hand and the grasped object compared with a full-actuated robot hand that has reduced DOF [5]. Therefore, the underactuated hands generally show better enveloping grasp stability than full actuated robot hands with reduced DOF.

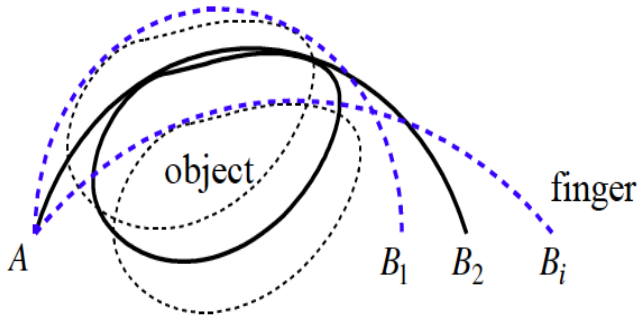

Figure 3: Enveloping grasp of underactuated compliant fingers.

This paper is organized as follows. In section 2, the shape stability of underactuated compliant fingers actuated by tendon-pulley systems is analyzed. In section 3, the robot hand prototype BFUH-2 is concisely introduced. In section 4, based on the operation modes analysis of human hands, the operation capability of underactuated compliant robot hands is analyzed and tested on the robot hand prototype. The conclusion of this paper is presented in section 5.

2. SHAPE STABILITY OF UNDERACTUATED FINGERS DRIVEN BY TENDON-PULLEY

Since the number of DOF of the mechanisms is more than that of the independent actuators, the shape stability of the underactuated compliant fingers is the important foundation of the enveloping grasp stability of underactuated multi-fingered hands. In this section, a sufficient condition is presented for underactuated finger mechanisms with three DOF when actuated by single actuator (see Figure **4**). Suppose the joint angles are $\theta_i, i=1,2,3$, the stiffness of the torsional springs is denoted by k_i, $i=1,2,3$, and the actuation force is F, then a proposition can be stated as follows.

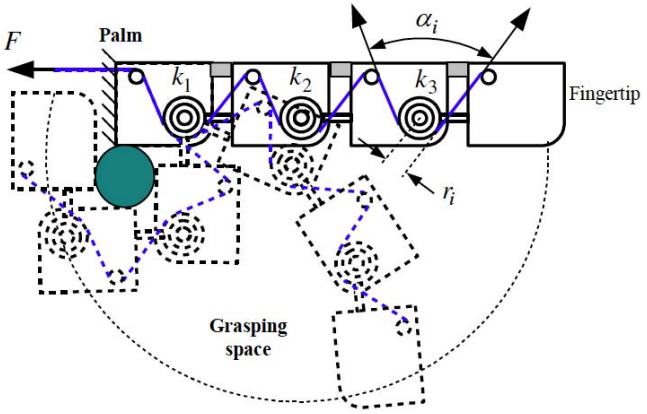

Figure 4: A planar underactuated finger mechanism with three DOF actuated by single tendon.

Proposition 1

For the planar underactuated finger mechanisms with three DOF actuated by single tendon, as shown in Figure **4**, where $\alpha_i, i=1,2,3$ is the included angle of the tendon on the pulley i. And $r_i>0$, $i=1,2,3$ denotes the valid radius of the pulleys, and each joint of the mechanism is installed a torsional spring with stiffness $k_i>0, i=1,2,3$, then the configurations of the underactuated compliant finger mechanism are always stable if all of the angles α_i satisfy $\alpha_i<\pi$, and the actuation force F is large sufficiently.

Proof

If the angle $\alpha_i, i=1,2,3$ always satisfy $\alpha_i<\pi$, then tendon is always contacting the pulleys with nonzero included forces. Thus, the tendon-pulley transmission system is valid for all configurations of the finger mechanism.

In this case, the actuation torque of the phalanx i is given by

$$\tau_i = Fr_i,\ i=1,2,3 \tag{1}$$

and the torque of the spring is given by

$$S_i = k_i\theta_i,\ i=1,2,3 \tag{2}$$

Suppose there is no friction in the joints, then the effective output torque of the joint i is

$$T_i = \tau_i - S_i = Fr_i - k_i\theta_i,\ i=1,2,3 \tag{3}$$

Since the actuation force F is sufficiently large, then it follows that

$$T_i \geq 0 \tag{4}$$

Thus, the configurations of the underactuated finger are stable for zero loads if $T_i=0$ and for nonzero loads if $T_i>0$. This completes the proof.

Remark 1

Applying the shape stability condition given by proposition 1, and combined with the condition

$$k_1 \leq k_2 \leq k_3 \tag{5}$$

the underactuated compliant finger presents the greatest grasping space as shown in Figure **4**, and shows the property of *progressive contacting* for objects with proper sizes as shown in Figure **5**. It is worth pointing out that the progressive contacting property of the underactuated fingers is rather important for improving the operation capability of the underactuated compliant robot hands. This important issue will be further analyzed in section 4.

3. A CONCISE INTRODUCTION OF THE ROBOT HAND PROTOTYPE BFUH-2

On the basis of the proposition 1, we have designed and fabricated a four-fingered underactuated robot hand prototype, which is illustrated in the Figure **6**. The total number of DOFs of the prototype is 12 while the number of independent actuators is 4, and the tendon-pulley transmission systems are adopted. The overall sizes of the hand prototype including the palm and the fingers are 0.238m in length, 0.180m in width and 0.034m in thickness. Thus, the hand prototype is slightly larger than the hand of a mature man. The weight of the hand is 0.92Kg that does not include the weight of the motors. The total weight of the prototype is 1.93Kg, which includes both the hand and the forearm. The total rated powers of the prototype are about 38 Watts, where the power of the thumb motor are 20 Watts and the power of the other figures is 6watts.

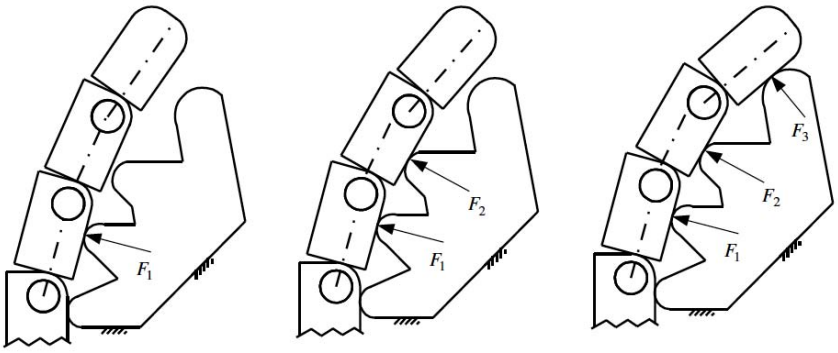

Figure 5: Progressive contacting of underactuated compliant grasping.

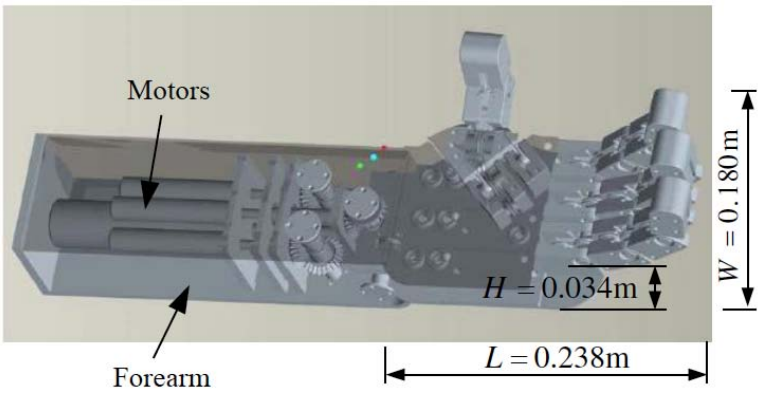

Figure 6: The four-fingered underactuated hand prototype.

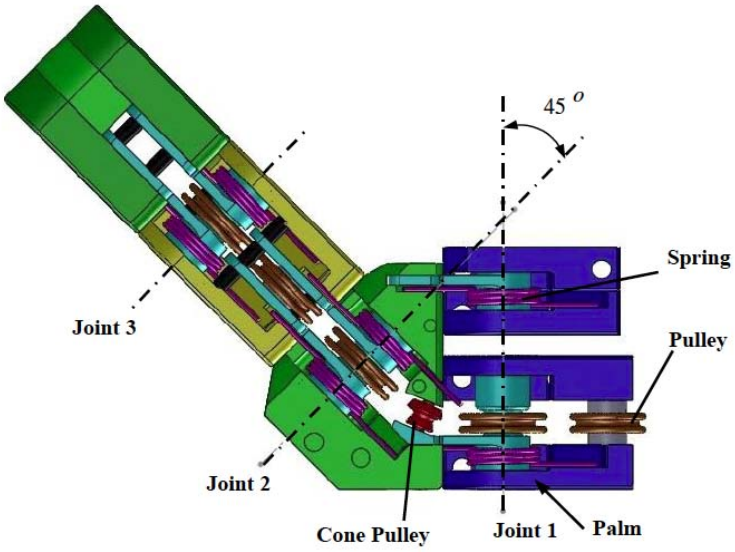

Figure 7: The 3D model of the thumb mechanism.

In order to show better anthropomorphic characteristics [19-21], the first and the second joint axis of the thumb intersect and the intersection angle is $\pi/4$ (see Figure **7**). As to the other three fingers, the mechanisms of them are designed as shown by Figure **4**. The 3D model of the index, middle and ring fingers are illustrated in Figure **8**. In the prototype, all of the torsional springs are alike and the stiffness of them is identically about $0.065\,Nm/Rad$.

The overall experiment system BFUH-2 is shown in Figure **9**. The main components of the system include the underactuated compliant robot hand prototype (see Figure **10a**), a subordinate controller (see Figure **10b**)

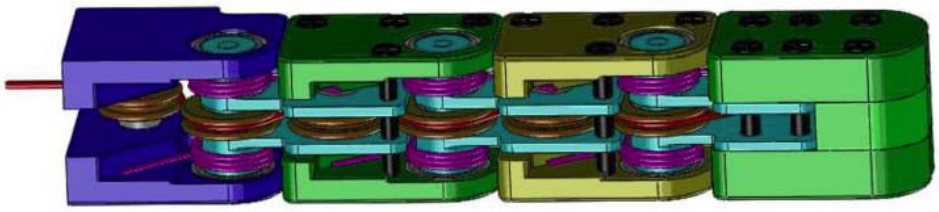

Figure 8: The 3D model of the index, middle and ring fingers.

and a host control computer. The function diagram of the subordinate controller is illustrated in Figure **11**. As shown in Figures **9** and **11**, an USB interface with maximum communication rate 2MPS is adopted as the primary communication mode between the subordinate controller and the host control computer.

In the subordinate controller, the main control chip is TMS320F2812 with 150MPS processing capability. The control software of the robot hand system in the host controller is written using the programming language Visual C++, and real time control algorithm of the closed-loop controller is written using the language

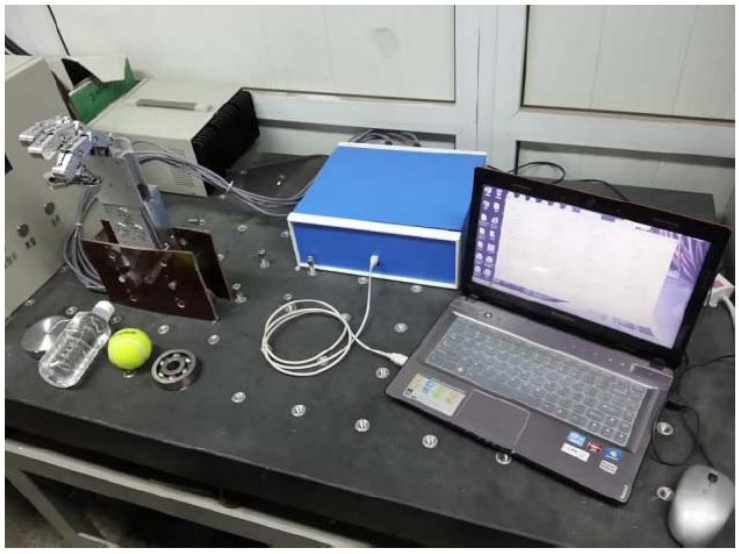

Figure 9: The experiment system BFUH-2.

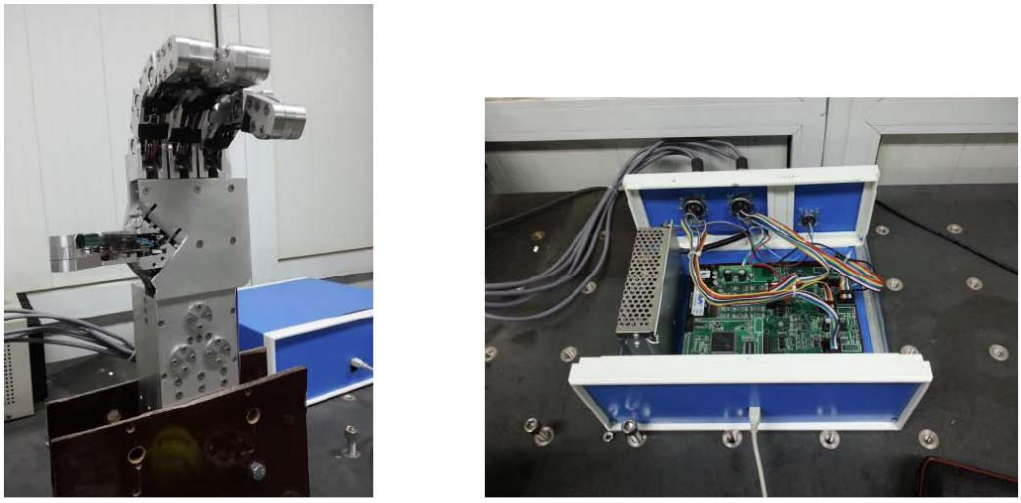

(a) Robot hand prototype (b) Subordinate Controller

Figure 10: The main components of the robot hand system.

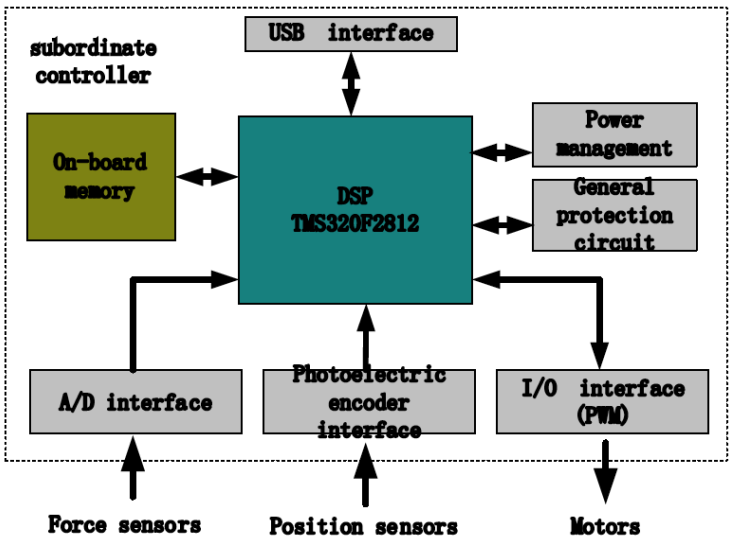

Figure 11: The function diagram of the subordinate controller.

C and finally downloaded to the on-board memory. In order to improve the state monitoring ability of the control system, four small force sensors are respectively installed on the inside surfaces of the fingertips. The resolution of A/D converters used in the subordinate controller is 12-bits, and DC motors in the system are controlled on the basis of Pulse Width Modulation (PWM) techniques.

4. OPERATION CAPABILITY ANALYSIS AND TEST OF THE PROTOTYPE

By observing the operations of our hands, the six primary sub-modes can be presented in Figure **12**, and the relevant sub-modes can be partitioned into two classes, namely *enveloping grasp mode* and *pinch mode*. The first class includes the sub-modes (a) to (d), which shows the distinguishing feature of catching big

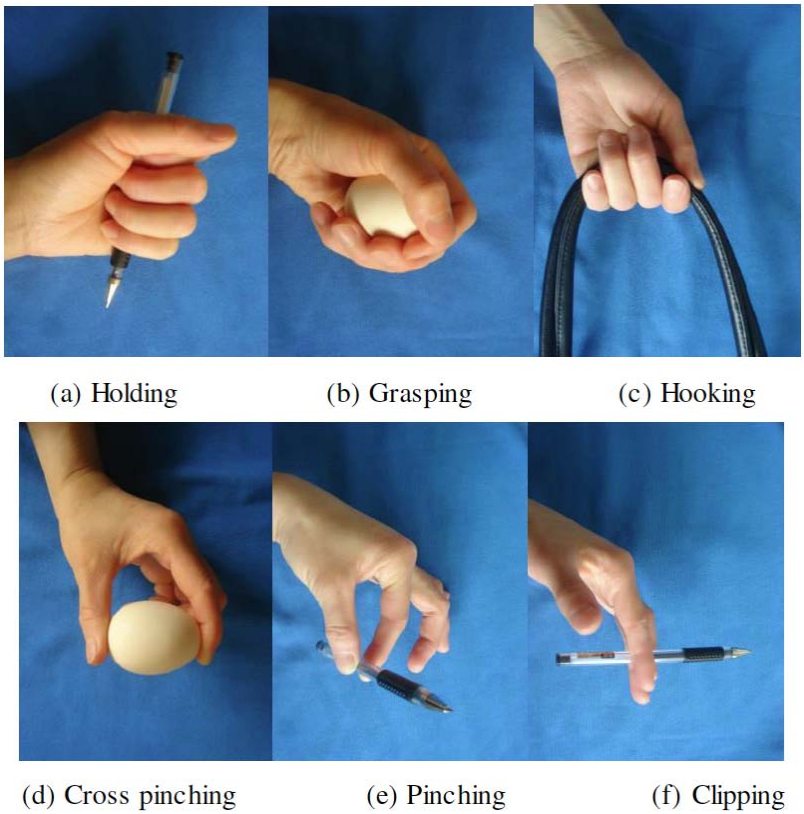

Figure 12: The main operation modes of human hands.

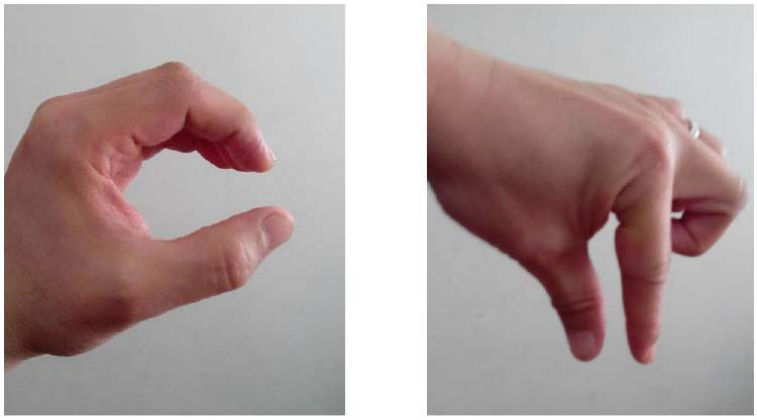

(a) Grasp mode (b) Pinch mode

Figure 13: Two primary classes of catch modes of human hands.

size objects. The second class includes the sub-modes (e) and (f) that shows how to catch small objects and the sub-mode (f) is relatively rarely used in our lives. So, the operation mode (f) has not been considered in designing the mechanical hands generally due to the relatively high system costs with regard to the relatively limited applications [18, 20].

4.1. Enveloping Grasp Stability Analysis and Relevant Experiments

For the two primary catch modes of our hands, as shown in Figure **13**, the grasp mode needs our fingers to form an envelope naturally (see Figure **13a**), so that enough contacting points between the hand and the object can be acquired. In this operation mode, the underactuated compliant fingers should form a set of *convex curves* [22] for given actuation forces. This indicates the stiffness of the torsional springs of the fingers should satisfy the relationship

$$k_1 = k_2 = k_3 \tag{6}$$

This means the stiffness of the joints of the underactuated fingers should be uniform, then for any actuation force and external force from object, the shapes of the fingers are always *convex plane curves* $\gamma_i(t)$, $i = 1,\ldots,4$ (the number of the fingers), and the *curvatures* (see Figure **14**) $\kappa_i(t) = \ddot{\gamma}_i(t) \neq 0$ along the curves $\gamma_i(t)$ are bounded to a relatively small range $|\kappa_i(t)| \in [\kappa_0 - \delta, \kappa_0 + \delta]$, where $\delta > 0$ is a small constant and $\kappa_0 > 0$ is a constant.

According to the design principle of (6) and proposition 1, the enveloping grasp operations can be fulfilled by the underactuated compliant robot hand shown in Figure **9** even though the force sensors of the prototype are not used in the feedback system. Figure **15** shows some experimental results of enveloping grasp operations of the prototype.

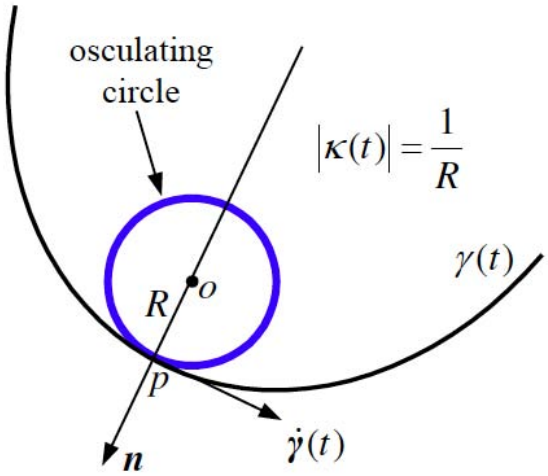

Figure 14: Curvatures of convex plane curves.

In Figure **15** the figures (a) to (d) are corresponding to the catch modes (a) to (c) of Figure **12**. As shown in Figure **15a**, a slender object can be stably grasped by the underactuated hand without any difficulties even if the thumb is not utilized in this operation. While for grasping a spherical object, such as the tennis ball shown in Figure **15b**, all of the fingers have to be used due to the relatively large size of the tennis ball. To grasp the bottle of water (see Figure **15c**), all of the fingers and large actuation forces have to be used since the weight of the object is rather large. As to grasp the glue gun (see Figure **15d**), thanks to the handle, this tool can be stably grasped. When the tea bucket (see Figure **15e**) is grasped, the thumb and the index finger are only used since the weight of the object is rather small. The operation of cross pinching

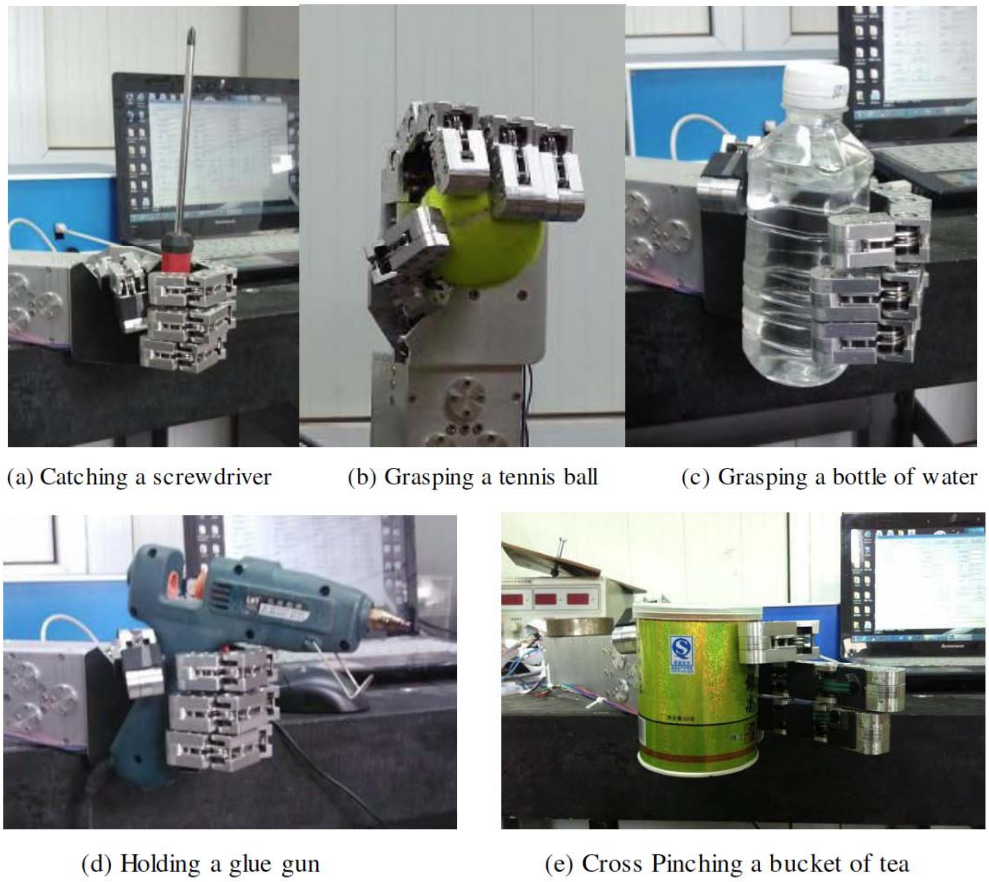

Figure 15: Enveloping grasp of the underactuated four-fingered robot hand prototype.

of the underactuated compliant hands for relatively big objects. On the basis of the analysis and experiments, the following proposition can be concluded.

Proposition 2

For a robot hand with three-phalanxes underactuated compliant fingers respectively actuated by single tendon-pulley actuator, in order to realize enveloping grasp operations, the stiffness of the three compliant joints in each finger should satisfy the relationship

$$k_1 \le k_2 \le k_3 \tag{7}$$

with the assumption of identical phalanxes in each underactuated compliant finger.

Proof

Here we use a proof by contradiction. Suppose the stiffness of the three compliant joints satisfies

$$k_1 > k_2 \tag{8}$$

or

$$k_2 > k_3 \tag{9}$$

Then the angular displacements of the compliant joints are not coincident with any given actuation force F. In these cases (8) and (9), the enveloping grasp spaces of the fingers reduce and the operations of the underactuated hands more easily cause ejection phenomena [1, 3]. Without losing the generality, for instance, as shown in Figure **16**, where the stiffness of the joints is based on the assumption $k_1 > k_2 > k_3$, the major deformation occurs in the last joint, so that the underactuated compliant fingers prematurely bend, then grasp operations can not be easily accomplished for the objects with even reasonable sizes. The proof is completed.

Remark 2

The proposition 2 gives a necessary condition to design the underactuated compliant robot hands for improving the operation capability of the systems. Following this design principle, the grasp operations of the underactuated compliant robot hands generally show the property of progressive contacting as shown in Figure **5**.

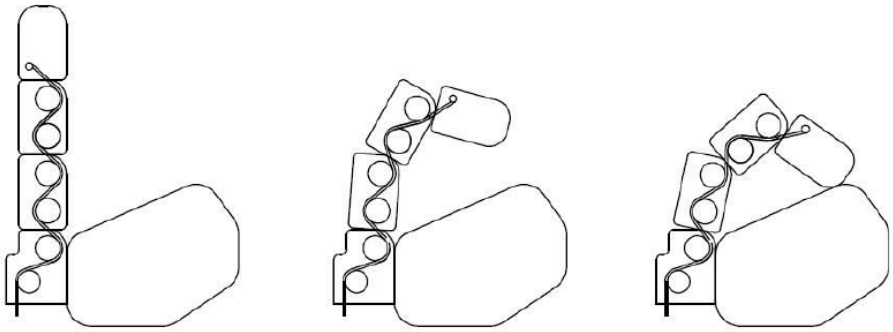

Figure 16: Ejection phenomena of a finger with improper stiffness in joints.

4.2. Pinch Stability Analysis of the Underactuated Compliant Robot Hands

In pinching mode of our hands as shown in Figure **13b**, the shape of our thumb and index finger can be approximated by a class of special convex plane curves that includes partial linear segments, as shown in Figure **17**. The curvatures of the convex plane curves related to the linear segments equal zero since the radius of the *osculating circle* [22] of the curve at the linear segment is infinite. For the underactuated fingers, the approximate linear segments should be the terminal part, so that the inside surfaces of the terminal phalanxes of thumb and the index finger could come into contacting. In this case, the thumb and the index finger become a gripper. On the basis of these observations, the following proposition is presented for the pinch operations of underactuated compliant robot hands.

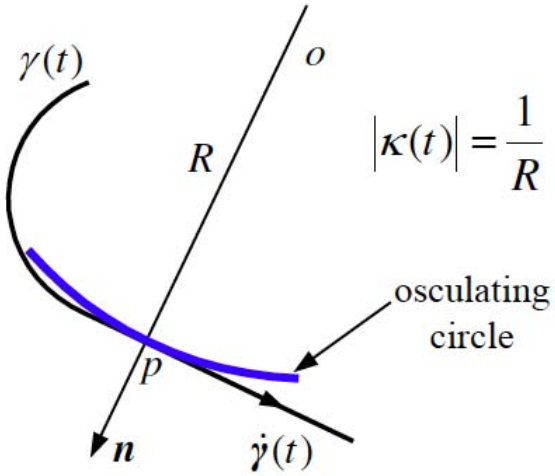

Figure 17: Curvatures of plane curve with linear segment.

Proposition 3

For a robot hand with three-phalanxes underactuated compliant fingers respectively actuated by single tendon-pulley actuator, in order to realize pinch operations, the stiffness of the three compliant joints of each finger should satisfy the relationship

$$k_1 < k_2 < k_3 \tag{10}$$

with the assumption of identical phalanxes in each underactuated compliant fingers.

Proof

Let's see Figure **13b**, in order to make the thumb and index finger work like a gripper, the primary deformation should occur in the first joint with regard to any given actuation force, then the stiffness of the torsional springs in the middle joint and the last joint should relatively higher than that of the first joint, since the effective actuation torques are almost identical in all joints of a finger. Similarly, to further improve the progressive contacting property of the underactuated compliant fingers, the stiffness of the last two phalanxes should satisfy the relationship $k_2 < k_3$.

The proof is completed.

Remark 3

The proposition 3 is also a necessary condition for designing the underactuated compliant robot hands that shows certain precision operation capabilities. In many precision operations, the multi-fingered robot hands have to pinch some small or flat objects, such as the discussion subject of the literature [23]. By the proposition 3, it is obvious that the curvatures of the approximate curves of the compliant fingers show a large variation range in this case.

It is a pity that precision operations cannot be completed by the prototype shown in Figure **10a** due to the relatively big size and the improper stiffness allocations of the underactuated compliant fingers. This research subject will be investigated in the future.

5. CONCLUSIONS

In this paper, we point out that multi-fingered robot hands possessing at least one elastic passive DOF can only be called the underactuated robot hands. To guarantee the controllability of the underactuated robot hands, passive DOF in robot hands should be elastic with certain stiffness. To design the underactuated compliant anthropomorphic robot hands actuated by tendon-pulley transmission systems, the stiffness of the torsional springs installed in the joints should satisfy certain conditions. In order to realize enveloping grasp operations, the stiffness of the first joint should not be higher than that of the last two joints. In order to implement precision operations, the stiffness of the first joint should be lower than that of the last two joints.

For the purpose of testing the operation capability of underactuated compliant robot hands, a four-fingered anthropomorphic robot hand prototype with underactuated compliant fingers had been fabricated on the basis of a principle of identical deformations of the compliant joints. By the robot hand prototype, some enveloping grasp experiments have been successfully accomplished with regard to relatively large objects, such as a screwdriver, a tennis ball, a bottle of water, a glue gun and a bucket of tea. Since the sizes of fingers of the prototype are relatively thick and big, and the stiffness of the joints is almost identical, many experiments with regard to small and flat objects have not been accomplished successfully.

Following the works presented in this paper, some suggestions are provided:

1. To improve the operation dexterity of the underactuated robot hands, the design of variable stiffness springs is a valuable research subject;

2. There generally exists a variety of different grasping methods in order to grasp a given object, so the motion planning of the underactuated compliant robot hands is another important research subject;

3. To improve the grasp stability of the underactuated compliant robot hands, the coordinated manipulations of manipulators and hands should be investigated in depth too.

ACKNOWLEDGEMENTS

This work is supported by the Natural Science Foundation of China with grants 51775002 and 11702294, the Joint Program of Beijing Municipal Foundation and Education Commission with grant KZ202010009015, and Beijing Natural Science Foundation with grant 3194047.

REFERENCE

[1] Birglen L, Laliberte T, Gosselin C. Underactuated Robotic Hands. New York: Springer- Verlag 2008. https://doi.org/10.1007/978-3-540-77459-4

[2] Birglen L, Gosselin C. Kinetostatic analysis of underactuated fingers. IEEE Transactions on Robotics and Automation 2004; 20(2): 211-221. https://doi.org/10.1109/TRA.2004.824641

[3] Birglen L, Gosselin CM. Grasp-state plane analysis of two-phalanx underactuated fingers. Mechanism and Machine Theory 2006; 41: 807-822. https://doi.org/10.1016/j.mechmachtheory.2005.10.004

[4] Licheng W, Carbone G, Ceccarelli M. Designing an underactuated mechanism for a 1 active DOF finger operation. Mechanism and Machine Theory 2009; 44: 336-348. https://doi.org/10.1016/j.mechmachtheory.2008.03.011

[5] Krut S, Begoc V, Dombre E, Pierrot F. Extension of the Form-Closure Property to Underactuated Hands. IEEE Transactions on Robotics 2010; 26(5): 853-866. https://doi.org/10.1109/TRO.2010.2060830

[6] Prattichizzo D, Malvezzi M, Gabiccini M, Bicch A. On the manipulability ellipsoids of underactuated robotic hands with compliance. Robotics and Autonomous Systems 2012; 60: 337-346. https://doi.org/10.1016/j.robot.2011.07.014

[7] Kragten GA, van der Helm FCT, Herder JL. A planar geometric design approach for a large grasp range in underactuated hands. Mechanism and Machine Theory 2011; 46: 1121-1136. https://doi.org/10.1016/j.mechmachtheory.2011.03.004

[8] Kragten GA, Herder JL. The ability of underactuated hands to grasp and hold objects. Mechanism and Machine Theory 2010; 45: 408-425. https://doi.org/10.1016/j.mechmachtheory.2009.10.002

[9] Touvet F, Daoud N, Gazeau J-P, Zeghloul S, Maier MA, Eskiizmirliler S. A biomimetic reach and grasp approach for mechanical hands. Robotics and Autonomous Systems 2012; 60: 473-486. https://doi.org/10.1016/j.robot.2011.07.017

[10] Kragten GA, Baril M, Gosselin C, Herder J. Stable Precision Grasps by Underactuated Grippers. IEEE Transactions on Robotics 2011; 27(6): 1056-1066. https://doi.org/10.1109/TRO.2011.2163432

[11] He G, Wang Z, Zhang J, Geng Z. Characteristics analysis and Stabilization of a planar 2R underactuated Manipulator Robitica 2014. https://doi.org/10.1017/S0263574714001714

[12] Adamek T, Kitts CA, Mas I. Gradient-Based Cluster Space Navigation for Autonomous Surface Vessels. IEEE/ASME Transactions on Mechatronics 2015; 20(2): 506-508. https://doi.org/10.1109/TMECH.2013.2297152

[13] Schultz G, Mombaur K. Modeling and Optimal Control of Human-Like Running. IEEE/ASME Transactions on Mechatronics 2010; 15(5): 783-792. https://doi.org/10.1109/TMECH.2009.2035112

[14] He G, Geng Z. Dynamics and Robust Control of an underactuated torsional Vibratory Gyroscope Actuated by Electrostatic Actuator. IEEE/ASME Transactions on Mechatronics 2014. https://doi.org/10.1109/TMECH.2014.2350535

[15] Murray RM, Li Z, Sastry SS. A Mathematical Introduction to Robotic Manipulation, London: CRC Press 1994.

[16] He G, Zhang C, Sun W, Geng Z. Stabilizing the Second-Order Nonholonomic Systems with Chained Form by Finite-Time Stabilizing Controllers. Robotica 2015. https://doi.org/10.1017/S0263574714002951

[17] Ozaw R, Kobayashi H, Hashirii K. Analysis, Classification, and Design of Tendon-Driven Mechanisms. IEEE Transactions on Robotics 2014; 30(2): 396-410. https://doi.org/10.1109/TRO.2013.2287976

[18] Peerdeman B, Valori M, Brouwer D, Hekman E, Misra S, Stramigioli S. UT hand I: A lock-based underactuated hand prosthesis. Mechanism and Machine Theory 2014; 78: 307-323. https://doi.org/10.1016/j.mechmachtheory.2014.03.018

[19] Mattar E. A survey of bio-inspired robotics hands implementation: new directions in dexterous manipulation. Robotics and Autonomous Systems 2013; 61: 517-544. https://doi.org/10.1016/j.robot.2012.12.005

[20] Yang D, Zhao J, Gu Y, Wang X, Li N, Jiang L, Liu H, Huang H, Zhao D. An Anthropomorphic Robot Hand Developed Based on Underactuated Mechanism and Controlled by EMG Signals. Journal of Bionic Engineering 2009; 6: 255-263. https://doi.org/10.1016/S1672-6529(08)60119-5

[21] Zollo L, Roccella S, Guglielmelli E, Chiara Carrozza M, Dario P. Biomechatronic Design and Control of an Anthropomorphic Artificial Hand for Prosthetic and Robotic Applications. IEEE/ASME Transactions on Mechatronics 2007; 12(4): 418-429. https://doi.org/10.1109/TMECH.2007.901936

[22] Klingenberg W. A course in differential geometry, New York: Springer-Verlag 1978. https://doi.org/10.1007/978-1-4612-9923-3

[23] Odhner LU, Ma RR, Dollar AM. Open-Loop Precision Grasping With Underactuated Hands Inspired by a Human Manipulation Strategy. IEEE Transactions on Automation Science and Engineering 2013; 10(3): 525-633. https://doi.org/10.1109/TASE.2013.2240298

Received on 10-11-2020 Accepted on 01-12-2020 Published on 31-12-2020

DOI: https://doi.org/10.31875/2409-9694.2020.07.4

© 2020 Xiao *et al*.; Zeal Press
This is an open access article licensed under the terms of the Creative Commons Attribution Non-Commercial License (http://creativecommons.org/licenses/by-nc/3.0/) which permits unrestricted, non-commercial use, distribution and reproduction in any medium, provided the work is properly cited.